Dissociative recombination of H_3^+: progress in theory

A. E. Orel, I. F. Schneider and A. Suzor-Weiner

Phil. Trans. R. Soc. Lond. A 2000 **358**, 2445-2456
doi: 10.1098/rsta.2000.0659

10.1098/rsta.2000.0659

Dissociative recombination of H_3^+: progress in theory

By A. E. Orel[1], I. F. Schneider[2,3] and A. Suzor-Weiner[3,4]

[1]*Department of Applied Science, University of California,*
Livermore, CA 94550, USA
[2]*National Institute for Lasers, Plasma and Radiation Physics,*
Bucharest-Măgurele, Romania
[3]*Laboratoire de Photophysique Moléculaire, Université Paris-Sud,*
F-91405 Orsay, France
[4]*Laboratoire de Chimie Physique, 11 rue Pierre et Marie Curie,*
F-75234 Paris, France

Dissociative recombination is the main destruction process for ground-state H_3^+ in diffuse interstellar medium. Experiments agree on relatively large cross-sections for this reaction. Time-dependent two-dimensional calculations confirm the experimental results at high energy as well as the observed predissociation rates of H_3 Rydberg states, due to non-adiabatic interactions. However, the value for low-energy cross-section, deduced from the predissociation rates by an extrapolation procedure, is about four orders of magnitude lower than the measured one. A calculation based on multichannel quantum defect theory suggests that an indirect non-adiabatic process may prevail in this case. The cross-section increases by orders of magnitude compared with the extrapolated value when indirect couplings via apparently ineffective channels are properly considered. We discuss how this channel-mixing mechanism can be effective in the case of H_3^+, and show encouraging results stressing the role of Rydberg series or 'closed channels'. We also discuss possible three-dimensional effects that could enhance the process at low energy.

Keywords: Rydberg states; interstellar molecules; dissociative recombination; non-adiabatic interactions; predissociation; molecular ion

1. Introduction

The dissociative recombination reaction,

$$M^+ + e^- \rightarrow \text{neutral fragments}, \tag{1.1}$$

is the dominant destruction process of molecular ions M^+ in cold plasmas with high electron densities. Such plasmas occur in diffuse interstellar clouds of molecules, planetary atmospheres, supernovae, as well as at the walls of fusion devices (Larsson *et al.* 2000). The neutral fragments produced by the reaction (1.1) are atoms or (if M^+ is a polyatomic ion) molecules usually in an excited state and may initiate chains of reactions that would be energetically forbidden with ground-state reactants. The dissociative recombination (DR) thus appears as a key reaction for the chemistry of ionized media, in particular for astrochemistry.

Phil. Trans. R. Soc. Lond. A (2000) **358**, 2445–2456

The case of H_3^+ has been, and still is, an enigma. The experimental history is described in this issue by Larsson. A very small upper limit was assigned to the rate for H_3^+ DR around 1984, based on experimental investigation using the FALP technique (Smith & Adams 1984). It was estimated to be less than 10^{-11} cm^3 s^{-1} at low temperature, that is about four orders of magnitude less than most usual DR rates. This small value was supported by theoretical estimates based on the unfavourable Franck–Condon overlap between the ion ground state and any dissociative state of the neutral molecule H_3 (Kulander & Guest 1979; Michels & Hobbs 1984). However, in 1989, a single-pass merged-beams experiment (Yousif & Mitchell 1989) measured a much faster rate (*ca.* 10^{-8} cm^3 s^{-1}), which was then found to be still faster (*ca.* 10^{-7} cm^3 s^{-1}) a few years later by multi-pass storage-ring measurements (Larsson *et al.* 1993) as well as in flowing afterglow discharge experiments (Laubé *et al.* 1998). Most of the experiments finally agreed on a value close to *ca.* 10^{-7} cm^3 s^{-1} at $T = 100$ K, which has been used in interstellar modelling. However, some plasma-type studies (Smith & Španel 1993; Gougousi *et al.* 1995) measured rates smaller by one order of magnitude. Some doubts still persist (Gougousi *et al.* 1995) about the influence of the inherent electric fields on the recombination process, which could result in an overestimation of the field-free thermal rates.

The merged-beams experiments have also measured branching ratios between the three-body $(H + H + H)$ and two-body $(H + H_2)$ dissociation. The three-body dissociation path represents 75% of the total DR cross-section at thermal energies, decreasing progressively to *ca.* 30% around 6 eV and becoming dominant again at higher energies.

Surprisingly, the H_3^+ column densities in both diffuse and dense interstellar regions were found to be large and of the same order of magnitude. This is hard to explain with a fast DR rate, since much less H_3^+ should survive DR in diffuse clouds than in dense ones, due to a much higher electron density. This is part of the enigma around H_3^+ DR. Another unsolved puzzle is the lack of theoretical quantitative explanation to date for the fast DR rate measured.

In § 2 we summarize the results of cross-section calculations for recombination with fast electrons (1–12 eV) using a time-dependent approach (Orel 2000). In this energy region, DR may proceed by its most usual (and most efficient) mechanism, with a direct electronic interaction between the ion-plus-electron initial complex and a dissociative surface of the neutral molecule. Experiment and theory agree on relatively large values for the DR cross-section and rate. Section 3 deals with the low-energy region, close to the ionization threshold and far from any dissociative valence state. Here, we have to rely on non-adiabatic interactions between non-crossing potential surfaces, much as for the case of HeH^+ DR, which has been studied theoretically for the last few years (Guberman 1994; Sarpal *et al.* 1994). A non-adiabatic coupling with the dissociative ground-state surface of H_3 explains well the predissociation observed for various Rydberg states below threshold (Schneider & Orel 1999), but extrapolation of this mechanism into the continuum leads to a much lower value for the cross-section than in the experiments. Section 4 explores other mechanisms, via indirect interaction with a series of bound Rydberg states.

2. The high-energy region

Quantum chemistry calculations (Kulander & Guest 1979; Michels & Hobbs 1984; Orel & Kulander 1993) have shown that doubly excited dissociative states cross the ionic electronic potential more than 1 eV *above* the H_3^+ ground vibrational state (threshold) in C_{2v} geometry. The lowest of the corresponding potential surfaces correlates diabatically to the ion-pair ($H_2^+ + H^-$) limit and adiabatically to the lowest ($H_2 + H$ $(n = 2)$) limit, situated 0.974 eV above threshold. Electrons with at least this kinetic energy may, thus, recombine directly into dissociative states through efficient electronic couplings, as in the case of most diatomic ions.

The strengths of these couplings have been evaluated by Orel & Kulander (1993) and, together with the energies of the relevant states, have been used to perform a time-dependent wave packet (TDWP) calculation (Heller 1978; Kulander & Heller 1978; Orel & Kulander 1989) of the DR cross-section above 1 eV (Orel & Kulander 1993).

The wave packet method proceeds by the direct integration of the time-dependent Schrödinger equation. Using the Jacobi coordinates (r, R, θ) and working within the C_{2v} symmetry, $\theta = 90°$, this equation becomes, for the DR of H_3^+ into a doubly excited dissociative state of potential energy $U_{\mathrm{diss}}(r, R)$:

$$\mathrm{i}\hbar\frac{\partial}{\partial t}\varPsi(r,R;t) = \{\boldsymbol{T}(r,R) + U_{\mathrm{diss}}(r,R) - \mathrm{i}\pi[V^{(\mathrm{el})}(r,R)]^2\}\varPsi(r,R;t). \tag{2.1}$$

Here, $\boldsymbol{T}(r, R)$ is the nuclear kinetic energy operator, $V^{(\mathrm{el})}(r, R)$ is the electronic coupling between the ionization and dissociation continua, and the complex imaginary term appearing in the Hamiltonian accounts for autoionization of the dissociative state.

The initial wave packet is given by the action of the electronic coupling on the vibrational eigenfunction of the target ion:

$$\varPsi(r,R;t=0) = V^{(\mathrm{el})}(r,R)\chi_{v_{\mathrm{s}}}(Q_{\mathrm{s}})\chi_{v_{\mathrm{b}}}(Q_{\mathrm{b}}), \tag{2.2}$$

the latter being approximated as the product of the harmonic oscillator wave functions $\chi_{v_{\mathrm{s}}}(Q_{\mathrm{s}})$ and $\chi_{v_{\mathrm{b}}}(Q_{\mathrm{b}})$ in the symmetric stretch and bending normal modes of H_3^+.

The DR cross-section is evaluated using the formula (in atomic units)

$$\sigma = (2\pi^3/\varepsilon)(\tfrac{1}{2}g)S(E), \tag{2.3}$$

where ε is the energy of the incident electron, E is the total energy, i.e. the sum of ε and the initial energy of the target ion, and g is the ratio of the multiplicities of the neutral and ion states. S is calculated by projecting the propagated wave function $\varPsi(r, R; t)$ for large times on the asymptotic channel eigenfunctions (Kulander & Heller 1978). When the final products of the dissociation are an atom and a diatomic molecule in the vibrational level v, we can define $S_2(E)$ (two-body) as

$$S_2(E) = \frac{m_R}{2\pi k}\sum_v \lim_{t\to\infty}\left|\iint \phi_v(r)\mathrm{e}^{\mathrm{i}kR}\varPsi(r,R;t)\,\mathrm{d}r\mathrm{d}R\right|^2, \tag{2.4}$$

where $\phi_v(r)$ is a vibrational wave function of H_2, $\mathrm{e}^{\mathrm{i}kR}$ is the plane wave describing the relative motion along the R coordinate between H and H_2, and m_R is the reduced mass associated to this motion. Once the sum in equation (2.4) is extended to include the continuum states of H_2, the result is the total DR cross-section.

This formalism allowed the first successful modelling of the H_3^+ and D_3^+ DR, and the main results are shown in figure 1. The theoretical cross-sections, including the

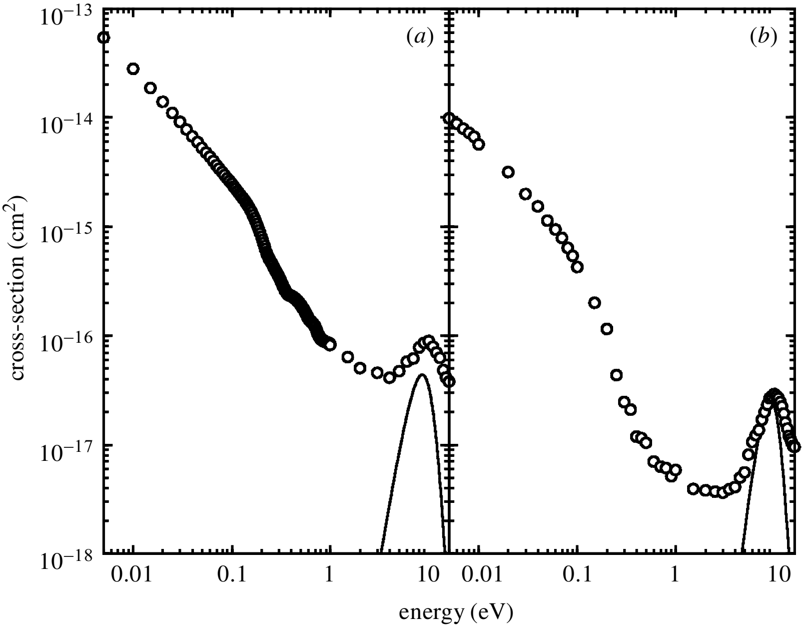

Figure 1. (*a*) H_3^+ and (*b*) D_3^+ DR cross-section. Circles denote experimental data obtained with CRYRING (Larsson *et al*. 1993, 1997). The solid line denotes theoretical results for high energy, based on the TDWP method (Orel & Kulander 1993) (see text).

contribution of four doubly excited states, reproduce the experimental peaks around 10 eV quite well. However, they fall dramatically outside the peak region, leaving the large experimental cross-sections unexplained in the low-energy range.

3. The low-energy region

(*a*) *Which mechanism?*

Since the doubly excited states are closed for dissociation below 0.974 eV, the only available dissociation channel at low energy is the ground state, whose potential surface *does not cross* that of the ion. For many years, this fact has been considered as an indication of a very low DR rate at thermal energies due to a small overlap of the nuclear wave functions, in contradiction with the high measured rates. In addition, no electronic interaction may couple the H_3 ground state and the lowest ionization continuum, which differ by only one spin-orbital.

However, an example has recently been found of relatively fast DR in a similar situation, for the HeH^+ ion. Here also, no low-lying valence state may dissociate the molecular system formed by the ion ground state and a slow electron, but non-adiabatic interaction with dissociative Rydberg states has proved to be effective. Although their potential curves do not cross the ion curve, three independent calculations (Guberman 1994; Sarpal *et al.* 1994; Tanabe *et al.* 1998) have shown that these Rydberg states lead to a relatively fast DR process, in good agreement with merged-beam measurements (Yousif & Mitchell 1989; Strömholm *et al.* 1996; Tanabe *et al.* 1998).

Based on these studies, we have explored the same mechanism for the case of H_3^+ DR. Since the DR of a ground-state ion is strongly related to the predissociation of Rydberg states converging to the same ion state (see § 3 *c*), we started by studying the predissociation of H_3 Rydberg states—for which many experimental data are available (Helm 1993; Müller & Cosby 1996)—in view of a later extension of the same formalism to the DR calculation.

(*b*) *The predissociation of* H_3

Predissociation is a non-radiative transition from a bound to a dissociative state. In the case of the low Rydberg states of H_3, this transition is attributed to the (dissociative) ground state. It results from a breakdown of the Born–Oppenheimer approximation, due to a kinetical coupling between the adiabatic molecular states. If we label two of these electronic states by $\mathit{\Psi}_i$ and $\mathit{\Psi}_j$, the main part of the non-adiabatic coupling is given by the operator

$$\boldsymbol{V}_{i,j}^{(\mathrm{na})} = -\frac{\hbar^2}{m_r}\langle \mathit{\Psi}_i|\frac{\partial}{\partial r}|\mathit{\Psi}_j\rangle\frac{\partial}{\partial r} - \frac{\hbar^2}{m_R}\langle \mathit{\Psi}_i|\frac{\partial}{\partial R}|\mathit{\Psi}_j\rangle\frac{\partial}{\partial R} - \frac{\hbar^2}{I}\langle \mathit{\Psi}_i|\frac{\partial}{\partial \theta}|\mathit{\Psi}_j\rangle\frac{\partial}{\partial \theta}, \tag{3.1}$$

where the matrix elements represent integration over electronic coordinates only. In the above formula, m_r is the reduced mass associated to the internuclear motion along r, and I is the momentum of inertia.

We have applied the analytic gradient technique (Lengsfield & Yarkony 1992) to evaluate the non-adiabatic matrix elements, i.e. the bra–kets in equation (3.1), relevant for the couplings between the 2p($^2E'$) ground state of H_3 and the 2s, 3s, 4s($^2A_1'$) and 3p($^2E'$) Rydberg states. The calculations were carried out on a three-dimensional grid that spanned the Franck–Condon region for the ground vibrational state of the H_3^+ ion.

The non-adiabatic coupling being determined, we used the technique described in § 2 to solve the time-dependent Schrödinger equation for propagation on the *ground-state* surface in two dimensions, i.e. for $\theta = 90°$, $C_{2\mathrm{v}}$ symmetry, and for the case of zero total angular momentum (Schneider & Orel 1999). More specifically, in equation (2.2) the vibrational wave function of the predissociating H_3 Rydberg state was approximated with that of the H_3^+ ion corresponding to the same vibrational quantum number, and the function $V^{(\mathrm{el})}(r,R)$ was replaced with the operator $\boldsymbol{V}^{(\mathrm{na})}(r,R)$ (equation (3.1)), corresponding to the non-adiabatic interaction between the Rydberg and the ground states (the indices i and j will be omitted from now on).

The rate α, lifetime τ and width $\mathit{\Gamma}$ for the predissociation of a state having the total (electronic plus vibrational) energy E are defined by

$$\alpha = \frac{1}{\tau} = \frac{\mathit{\Gamma}}{\hbar} = \frac{2\pi}{\hbar}S(E), \tag{3.2}$$

where $S(E)$ is given either by equation (2.4), or by performing the Fourier transform of the overlap between the propagated and initial wave function (Heller 1978):

$$S(E) = \int_{-\infty}^{\infty} \mathrm{e}^{\mathrm{i}Et/\hbar}\langle \mathit{\Psi}(r,R;t=0)|\mathit{\Psi}(r,R;t)\rangle\,\mathrm{d}t. \tag{3.3}$$

We have evaluated predissociation rates for the ground vibrational levels of the 2s($^2A_1'$), 3s($^2A_1'$) and 3p($^2E'$) states, and for the first excited symmetric stretch mode

Table 1. *Predissociation rates of* H_3 *and* H_3 *Rydberg states*

			theory		experiment	
	state[a]	energy (eV)[b]	two-body rate (10^7 s^{-1})	three-body rate (10^7 s^{-1})	two-body rate (10^7 s^{-1})[c]	total decay rate (10^7 s^{-1})[d]
H_3	2s $^2A'_1(0,0)$	5.449	5.7×10^4			5.65×10^5
	3p $^2E'(0,0)$	7.194	7.9×10^2	1.77×10^3		
	3s $^2A'_1(0,0)$	7.634	8.2	4.2	7.1	$\cdots < 9.4$
						$1.0 < \cdots < 5.0$
						$2.5 < \cdots < 12.5$
	3s $^2A'_1(1,0)$	8.031	44	29	4–40[e]	
D_3	2s $^2A'_1(0,0)$	5.348	8.65×10^3			
	3p $^2E'(0,0)$	7.093	21	38		
	3s $^2A'_1(0,0)$	7.533	0.2	0.06		
	3s $^2A'_1(1,0)$	7.819	1.6	0.4		

[a] The vibrational quantum numbers of the symmetric stretch and bending mode are indicated in the parentheses; the angular quantum numbers are $N = 1$ and $K = 0$.

[b] Relative to H_2 $^1\Sigma_g^+$ $(v = 0)$ + H $(n = 1)$.

[c] From Müller & Cosby (1996).

[d] The total decay rate is the sum of the rates for radiative decay and two- and three-body predissociation.

[e] According to U. Müller (personal communication).

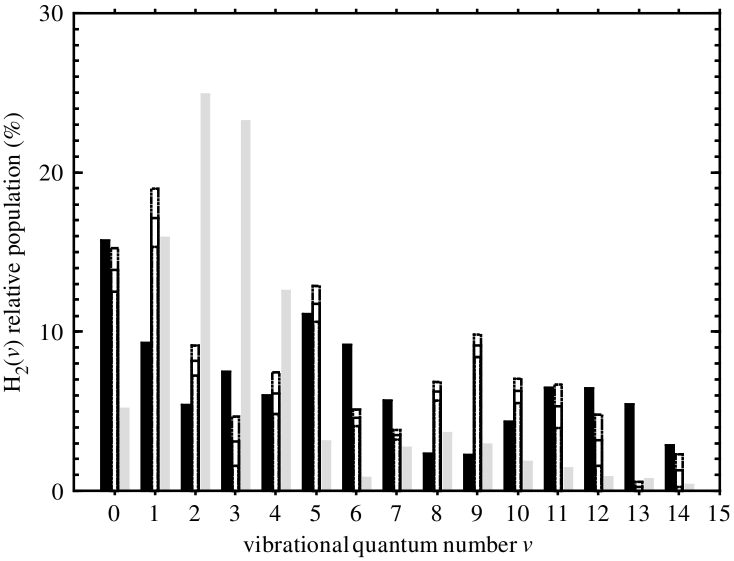

Figure 2. Relative vibrational populations in the H_2 $^1\Sigma_g^+(v)$ fragments produced by the predissociation of the (v_s = 1, v_b = 0) vibrational states of the 3s $^2A'_1$ Rydberg level of H_3 ($N = 1$, $K = 0$). The present calculations are marked with solid bars, calculations with the non-adiabatic coupling operator equal to unity are marked with grey bars. The open bars represent the results obtained by Müller & Cosby (1996) (the dotted lines mark the experimental error bars).

of the $3s(^2A_1')$ state. The computed rates, shown in table 1, are in satisfactory agreement with the measured ones (Müller & Cosby 1996).

Even more encouraging is the reasonable agreement between our estimations and the experimental data on the vibrational distributions of the $H_2\,{}^1\Sigma_g^+$ dissociation product. As shown in figure 2, the present theory qualitatively confirms the relative populations of the low vibrational levels, as well as the overall shape of this distribution. The theoretical predictions assuming a constant non-adiabatic coupling are also displayed for comparison.

(*c*) *The direct DR of* H_3^+

The predissociated states studied above belong to Rydberg series that can be extended into the ionization continuum. In particular, for high principal quantum numbers n, these couplings scale (in atomic units) as

$$\langle \Psi_{\mathrm{continuum}} | \frac{\partial}{\partial R} | \Psi_{\mathrm{gd}} \rangle = \langle \Psi_{\mathrm{Rydberg}} | \frac{\partial}{\partial R} | \Psi_{\mathrm{gd}} \rangle (n - \mu(r, R, \theta))^{1.5}, \tag{3.4}$$

where $\mu(r, R, \theta)$ is the quantum defect and Ψ_{gd}, Ψ_{Rydberg} and $\Psi_{\mathrm{continuum}}$ are the electronic wave functions associated with the ground state, the Rydberg predissociated state, and a state from the ionization continuum, respectively.

Consequently, for each of these series, we can evaluate the contribution of the corresponding partial wave of the incident electron to the *direct* DR, where the incident electron is directly captured into a dissociative state of the neutral molecule, the ground state in the case of H_3. The DR cross-section is evaluated using equation (2.3), $S(E)$ being obtained as described in § 3 *b*, the main difference with respect to the predissociation study being the use of the *scaled* non-adiabatic matrix elements (equation (3.4)) in formula (3.1). The 'scaled' $\boldsymbol{V}^{(\mathrm{na})}(r, R)$ operator plays the same role as the electronic one $V^{(\mathrm{el})}(r, R)$ relevant for the high-energy region (§ 2). Note, however, that at low energy, the autoionization of the dissociative state cannot be accounted for by a complex imaginary term added to the actual potential energy $U_{\mathrm{diss}}(r, R)$, since $\boldsymbol{V}^{(\mathrm{na})}(r, R)$ is a *non-local operator*, rather than a *function* as $V^{(\mathrm{el})}(r, R)$ is. We therefore disregarded autoionization at this stage of our analysis.

Following this procedure, we have obtained for H_3^+ and D_3^+ the DR cross-sections displayed in figure 3 (only the s and p series have been treated, since the non-adiabatic couplings corresponding to the d series are significantly smaller). Whereas for predissociation our results agree well with the measurements, in the case of DR we face a disagreement of orders of magnitude! However, this result is not surprising: the position of the neutral dissociative state with respect to the molecular ion surface (Kulander & Guest 1979; Michels & Hobbs 1984) corresponds to a very low Franck–Condon factor, much lower than in the case of HeH^+ DR, which was found to be relatively fast (Guberman 1994). Here, the direct DR *has to be slow*, and our calculation is just one of the necessary steps towards its complete modelling. We have to consider other mechanisms that, in the case of the H_3 system, could be more efficient than direct DR in the C_{2v} symmetry.

4. The role of the indirect process

Besides the direct capture of the incident electron into a repulsive state of the neutral molecule, DR may also proceed by a two-step mechanism, called *indirect* DR.

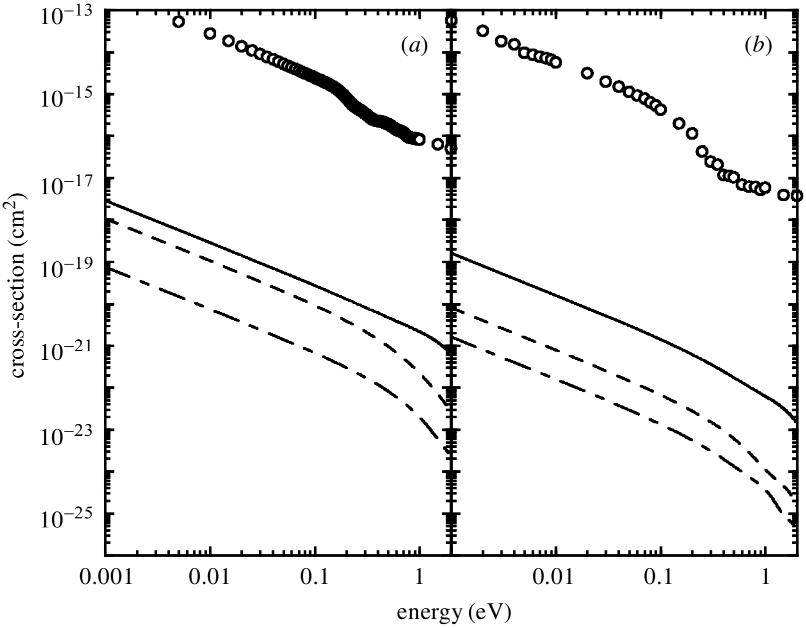

Figure 3. DR of (a) H_3^+ and (b) D_3^+ at low energy, modelled within a wave packet approach. Lines denote computed direct cross-sections, corresponding to s $^2A_1$ (dot–dashed), p $^2A_1$ (dashed), and p $^2B_2$ (solid) continua of the 'ion-plus-electron' system, described in the C_{2v} symmetry. Circles denote CRYRING measurements (Larsson *et al.* 1997).

First, a bound state (usually a Rydberg state) is populated by electron capture into an excited energy level lying above the ionization threshold. Fragmentation of the neutral molecule then occurs by predissociation of this state. Both electron capture and predissociation may involve various types of interaction (electronic, non-adiabatic, spin-orbit, etc.), much as for the direct process. The two mechanisms, direct and indirect, usually coexist and interfere. With notable exceptions (e.g. HeH^+ (Guberman 1994) and He_2^+ (Carata *et al.* 1999)), the fast direct DR is setting the order of magnitude of the cross-section, while the indirect process is responsible for resonance structures that hardly affect the value of the DR rate. However, if the direct DR is very slow, the cross-section may actually increase by orders of magnitude (Guberman 1994; Schneider *et al.* 2000*a*, *b*; Schneider & Suzor-Weiner 2000) when *indirect* couplings are included in a multichannel calculation. We show below that such a situation could help explain the fast DR cross-section measured for H_3^+ at low energy.

It has often been suggested that the indirect DR should play an important role in H_3^+ DR. Mechanisms involving temporary capture of the incident electron into 'low-n, high-v', or 'high-n, low-v' Rydberg H_3 states, subsequently predissociated by the ground state (Helm 1993; Canosa *et al.* 1992), have been proposed, as well as a multi-step indirect DR process involving a series of $\Delta v = 1$ transitions (Bates *et al.* 1993). However, until now no quantitative account of this effect has been given. At very low energy we are in the situation described above, with a very slow direct process (see figure 3) but rather strong non-adiabatic couplings between the initial ion continuum and bound Rydberg states on one hand, and between these Rydberg

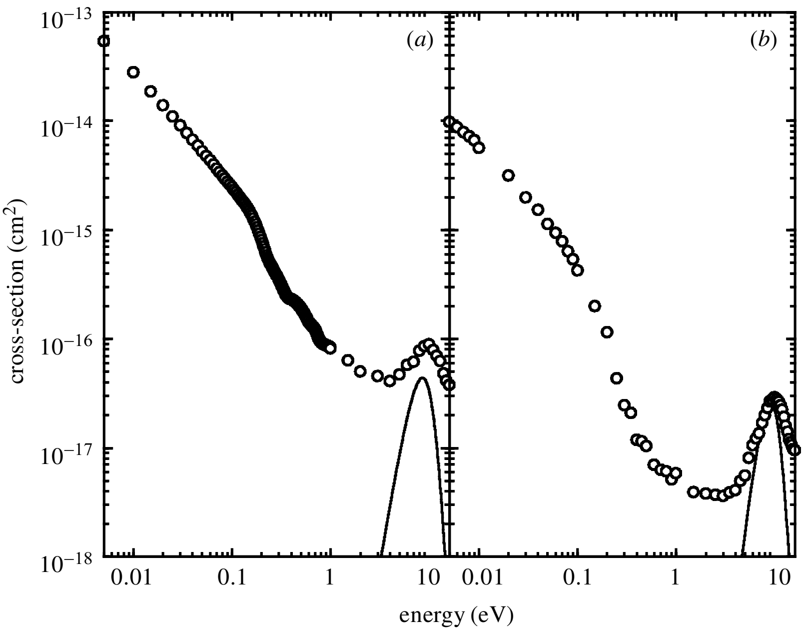

Figure 4. DR of H_3^+ at low energy, modelled within a combined MQDT–wave packet approach. The dashed black line denotes the computed direct cross-section. The grey line denotes the computed total (direct and indirect) cross-section. Circles denote CRYRING measurements (Larsson *et al.* 1997). The solid black line denotes the computed total cross-section, convoluted according to the anisotropic Maxwell distribution characterizing the ions in the CRYRING experiment (Larsson *et al.* 1997). The computations are performed in the C_{2v} symmetry and are restricted to the contribution of the $\mathrm{p}\,{}^2B_2$ continuum of the 'ion-plus-electron' system.

states and the repulsive ground state on the other hand. Since the dissociative nuclear wave function has a large overlap with highly excited vibrational wave functions of bound Rydberg states, the indirect process via 'closed' ionization channels (i.e. Rydberg series) may cause a spectacular enhancement of the DR process. Using the DR approach (Giusti-Suzor 1980) based on the multichannel quantum defect theory (MQDT), such an effect was demonstrated for similar situations in diatomics, e.g. HeH^+ (Guberman 1994) and HD^+ (Schneider *et al.* 2000*a*, *b*; Schneider & Suzor-Weiner 2000).

The MQDT treatment of the DR (Giusti-Suzor 1980) is not yet adapted for the polyatomic case, and the TDWP case is not yet able to account for the indirect process. Therefore, we have used a hybrid treatment as a first modelling of total (i.e. direct and indirect) DR of H_3^+. Specifically, the direct non-adiabatic couplings between the ionization channels, open and closed, and the dissociative ground state were evaluated using the TDWP technique, while the vibrational couplings between ionization channels were introduced via the channel mixing coefficients:

$$\langle \chi_{v_\mathrm{s}} \chi_{v_\mathrm{b}} | \cos[\pi\mu(r, R, \theta = 90^\circ)] | \chi_{v_{\mathrm{s}'}} \chi_{v_{\mathrm{b}'}} \rangle$$

and

$$\langle \chi_{v_\mathrm{s}} \chi_{v_\mathrm{b}} | \sin[\pi\mu(r, R, \theta = 90^\circ)] | \chi_{v_{\mathrm{s}'}} \chi_{v_{\mathrm{b}'}} \rangle .$$

Here, $\mu(r, R, \theta)$ is the quantum defect surface previously computed (Krause *et al.* 1992; Schneider & Orel 1999), and $|\chi_{v_s}\chi_{v_b}\rangle$ a two-dimensional ion vibrational wave function. An MQDT calculation of the low-energy total cross-section has been performed, restricted for now to the contribution of the p $^2B_2$ symmetry of the 'ion-plus-electron' system. The indirect process was accounted for through the inclusion of the *closed* channels (Giusti-Suzor 1980). The result is shown in figure 4: although the initial discrepancy between theory and experiment illustrated by figure 3 is not yet removed, the computed cross-section increases by two orders of magnitude, on average, when the indirect process is included. This clearly demonstrates its decisive *constructive* role in the case of the low-energy DR of H_3^+.

5. Conclusions and perspectives

Important progress has been made in the theoretical study of the dissociation dynamics of H_3 and its isotopomers. The calculated predissociation rates and the vibrational distributions of the dissociation products agree well with the existing experimental data. We have estimated the magnitude of the *direct* H_3^+ DR, and we have shown that this process is slow, as expected. MQDT modelling relying on the inclusion of the closed channels has shown that the *indirect* process is orders of magnitude more efficient than the direct one, a fact that might explain, at least partly, the high DR cross-sections at low *and* moderate energies.

Much work remains to be done for a satisfactory understanding and modelling of H_3^+ DR. Besides the account of the indirect process, other mechanisms, such as the actual opening of the doubly excited states for low-energy DR through an efficient coupling to the ground state, should be carefully examined.

A major approximation in our calculation is the restriction to two dimensions, $\theta = 90^\circ$, i.e. C_{2v} symmetry. For the high-energy calculations, where the dissociation proceeds via doubly excited states of the neutral, this is justified, since the dissociative potential energy surfaces are relatively flat with respect to changes in θ, but fall steeply in energy as r and R are increased. However, in the low-energy case this is not true. Consequently, the Franck–Condon overlaps could change considerably when passing from two to three dimensions (C_s symmetry), the corresponding change of couplings being quite able to alter the computed DR cross-section, direct and total. Moreover, the actual vibrational structure corresponding to a system described by three coordinates is much more dense than that accounted for in the present calculations, where only two vibrational modes were available.

Another consequence of extending our calculations to the three-dimensional case would be the more realistic and general account of the various available couplings. For example, in the equilateral (D_{3h}) configuration, the s states are of $^2A_1'$ symmetry and are coupled by the non-adiabatic coupling operator to the degenerate ground $^2E'$ state, whereas within C_{2v} symmetry these states are of $^2A_1$ symmetry and are coupled only to the $^2A_1$ sheet of the ground state, which converges asymptotically to the $H + H_2$ limit, and not to the $^2B_2$ sheet, which goes to the $H + H + H$ limit. Similarly, the p states should couple to the degenerate ground state, but, in C_{2v}, one couples to the $^2A_1$, the other to the $^2B_2$ sheet. Recent calculations performed to explain the optical emission spectra of H_3 and its isotopomers (Mahapatra & Köppel 1998*a*, *b*) have shown that the asymmetric stretch, that is changing θ, can produce significant effects. Such calculations must include both ground-state sheets and take into account the coupling between these sheets. These calculations are underway.

I.F.S. acknowledges support from the French CNRS, Université Paris VI, The Royal Society and NATO. A.E.O. acknowledges support from the National Science Foundation (grant no. PHY-97-22136) and the US Department of Energy by the University of California Lawrence Livermore National Laboratory (contract no. W-7405-Eng-48). This work was also supported by the French Institut National pour les Sciences de l'Univers.

References

Bates, D. R., Guest, M. F. & Kendall, R. A. 1993 *Planet. Space Sci.* **41**, 9.

Canosa, A. *et al.* 1992 *J. Chem. Phys.* **97**, 1028.

Carata, L., Orel, A. E. & Suzor-Weiner, A. 1999 *Phys. Rev.* A **59**, 2804.

Giusti-Suzor, A. 1980 *J. Phys.* B **13**, 3867.

Gougousi, T., Johnsen, R. & Golde, M. F. 1995 *Int. J. Mass. Spectrom. Ion. Proc.* **149/150**, 131.

Guberman, S. L. 1994 *Phys. Rev.* A **49**, R4277.

Heller, E. J. 1978 *J. Chem. Phys.* **68**, 2066, 3891.

Helm, H. 1993 In *Dissociative recombination: theory, experiment and applications*, II (ed. B. Rowe, J. B. A. Mitchell & A. Canosa), p. 145. New York: Plenum.

Krause, J. L., Orel, A. E., Lengsfield III, B. H. & Kulander, K. C. 1992 In *Time dependent quantum molecular dynamics: experiments and theory* (ed. J. Broeckhove & L. Lathouwers), p. 131. New York: Plenum.

Kulander, K. C. & Guest, M. F. 1979 *J. Phys.* B **12**, L501.

Kulander, K. C. & Heller, E. J. 1978 *J. Chem. Phys.* **69**, 2439.

Larsson, M. *et al.* 1993 *Phys. Rev. Lett.* **70**, 430.

Larsson, M. *et al.* 1997 *Phys. Rev. Lett.* **79**, 395.

Larsson, M., Mitchell, J. B. A. & Schneider, I. F. (eds) 2000 *Dissociative recombination: theory, experiment and application*, IV. Singapore: World Scientific.

Laubé, S. *et al.* 1998 *J. Phys.* B **31**, 2111.

Lengsfield III, B. H. & Yarkony, D. R. 1992 *Adv. Chem. Phys.* **82**, 1.

Mahapatra, S. & Köppel, H. 1998*a* *J. Chem. Phys.* **109**, 1721.

Mahapatra, S. & Köppel, H. 1998*b* *Phys. Rev. Lett.* **81**, 3116.

Michels, H. H. & Hobbs, R. H. 1984 *Astrophys. J.* **286**, L27.

Müller, U. & Cosby, P. C. 1996 *J. Chem. Phys.* **105**, 3532.

Orel, A. E. 2000 In *Dissociative recombination: theory, experiment and application*, IV (ed. M. Larsson, J. B. A. Mitchell & I. F. Schneider), p. 91. Singapore: World Scientific.

Orel, A. E. & Kulander, K. C. 1989 *J. Chem. Phys.* **91**, 6086.

Orel, A. E. & Kulander, K. C. 1993 *Phys. Rev. Lett* **71**, 4315.

Sarpal, B. K., Tennyson, J. & Morgan, L. A. 1994 *J. Phys.* B **27**, 5943.

Schneider, I. F. & Orel, A. E. 1999 *J. Chem. Phys.* **111**, 5873.

Schneider, I. F. & Suzor-Weiner, A. 2000 (In preparation.)

Schneider, I. F., Larsson, M., Orel, A. E. & Suzor-Weiner, A. 2000*a* In *Dissociative recombination: theory, experiment and application*, IV (ed. M. Larsson, J. B. A. Mitchell & I. F. Schneider), p. 131. Singapore: World Scientific.

Schneider, I. F., Orel, A. E. & Suzor-Weiner, A. 2000*b* In *Dissociative recombination: theory, experiment and application*, IV (ed. M. Larsson, J. B. A. Mitchell & I. F. Schneider), p. 295. Singapore: World Scientific.

Smith, D. & Adams, N. G. 1984 *Astrophys. J.* **284**, L13.

Smith, D. & Španel, P. 1993 *Int. J. Mass Spectrom. Ion. Proc.* **129**, 163.
Strömholm, C. *et al*. 1996 *Phys. Rev.* A **54**, 3086.
Tanabe, T. *et al*. 1998 *J. Phys.* B **31**, L297.
Yousif, F. B. & Mitchell, J. B. A. 1989 *Phys. Rev.* A **40**, 4318.

Discussion

J. B. A. Mitchell (*PALMS, Université de Rennes, France*). There was a question concerning possible field effects due to the downstream electric field in merged-beam experiments. If the H_3^+ recombination proceeds via a rotational interaction and produces a high n ($n \approx 30$) Rydberg state that is sufficiently long-lived (10s of seconds) to reach the bending magnet in a storage ring, or the electrostatic beam deflector in a single-pass merged-beam apparatus, then such states would be field ionized and the recombination event would not be seen. Such states would also be affected by collisions in afterglow experiments. If the recombination proceeds by a vibrational interaction, this could produce an $n = 7$ Rydberg state that would not be field ionized in the bending magnet nor in the electrostatic beam deflector ($3\,\mathrm{kV\,cm^{-1}}$ field). It could, however, be field dissociated by the bending magnet (motional electric field $10^5\,\mathrm{V\,cm^{-1}}$). This might affect the branching ratio.